1

Downloaded from http://aem.asm.org/ on August 22, 2018 by guest

Quorum sensing in Pseudomonas savastanoi pv. savastanoi and Erwinia 2 3 toletana: role in virulence and interspecies interactions in the olive knot 4 5 Eloy Caballo-Ponce<sup>1</sup>\*, Xianfa Meng<sup>2</sup>\*<sup>¶</sup>, Gordana Uzelac<sup>2</sup>, Nigel Halliday<sup>3</sup>, Miguel 6

Cámara<sup>3</sup>, Danilo Licastro<sup>4</sup>, Daniel Passos da Silva<sup>2‡</sup>, Cayo Ramos<sup>1+</sup>, and Vittorio 7 8 Venturi<sup>2+</sup>

9

12

Instituto de Hortofruticultura Subtropical y Mediterránea La Mayora, Universidad de 10

Málaga-Consejo Superior de Investigaciones Científicas, Málaga, Spain<sup>1</sup> 11

International Centre for Genetic Engineering and Biotechnology, Trieste, Italy<sup>2</sup> 13

14

15 School of Life Sciences, Centre for Biomolecular Sciences, University of Nottingham,

Nottingham, United Kingdom<sup>3</sup> 16

- 18 CBM S.c.r.l., Area Science Park-Basovizza, Trieste, Italy<sup>4</sup>
- 19

17

\* equal contribution 20

21 + co-corresponding - Vittorio Venturi, email: venturi@icgeb.org; Cayo Ramos, email:

- 22 crr@uma.es
- 23

¶ current address: Integrative Microbiology Research Centre, South China Agricultural 24

25 University, Guangzhou 510642, China

‡ current address: Department of Microbiology, University of Washington, Seattle, WA. 26

Accepted Manuscript Posted Online

29 ABSTRACT: The olive-knot disease (Olea europea L.) is caused by the bacterium 30 Pseudomonas savastanoi pv. savastanoi (PSV). PSV in the olive-knot undergoes 31 interspecies interactions with the harmless endophyte Erwina toletana (ET); PSV and ET 32 co-localize and form a stable community resulting in a more aggressive disease. PSV and 33 ET produce the same type of the N-acylhomoserine lactone (AHL) quorum sensing (QS) 34 signal and they share AHLs in planta. In this work we have further studied the AHL QS 35 systems of PSV and ET in order to determine possible molecular mechanism(s) involved 36 in this bacterial inter-species interaction/cooperation. The AHL QS regulons of PSV and 37 ET were determined allowing the identification of several QS-regulated genes. 38 Surprisingly, the PSV QS regulon consisted of only a few loci whereas in ET many 39 putative metabolic genes were regulated by QS among which several involved in 40 carbohydrate metabolism. One of these loci was the aldolase-encoding gene garL, which 41 resulted to be essential for both co-localization of PSV and ET cells inside olive knots as 42 well as knot development. This study further highlighted that pathogens can cooperate 43 with commensal members of the plant microbiome.

44 SIGNIFICANCE OF THIS STUDY: This is a report on studies of the quorum sensing 45 (QS) systems of olive knot pathogen Pseudomonas savastanoi pv. savastanoi and olive-46 knot cooperator Erwinia toletana. These two bacterial species form a stable community 47 in the olive knot, share QS signals and cooperate resulting in a more aggressive disease. 48 In this work we further studied the QS systems by determining their regulons as well 49 studying QS-regulated genes which might play a role in this cooperation. This represents 50 a unique in vivo interspecies bacterial virulence model and highlights the importance of 51 bacterial interspecies interaction in disease.

### 53 INTRODUCTION

54 The recent dramatic increase of microbiome studies has further evidenced what microbiologists have postulated for many years, that most commonly, microorganisms in 55 nature live as members of complex multispecies communities (1, 2). This has 56 57 demonstrated that many different microbes live in close proximity to each other; however, 58 aspects of microbe-microbe interactions have thus far been significantly understudied. In 59 addition, multispecies microbial communities existing in association with plants could be 60 influenced by the plant and/or could have consequences on plant health; again very few 61 studies have investigated this likely scenario.

62 Many bacterial species have been studied for their intraspecies signaling system which is 63 known as quorum sensing (QS) (3). QS involves the production and detection of signal molecules which results in the regulation of gene expression in response to bacterial cell 64 65 number/density (4). Gram-negative bacteria most commonly use N-acylhomoserine 66 lactones (AHLs) as QS signals and in proteobacterial phytopathogens it is involved in the 67 regulation of expression of virulence associated factors in the plant (5-9). An archetypical 68 AHL QS system consists of a LuxI-family AHL synthase and a LuxR-family 69 transcription factor which affects target gene expression upon interaction with the 70 cognate AHL at quorum concentrations (10). AHLs vary in their structure having different acyl chain lengths (from 4 to 20 carbons) and display differences in their 71 72 oxidation state at position C3. AHL signals can also be involved in interspecies signaling 73 in a community since they are freely diffusible and can thus be detected by different 74 bacterial neighbors. In bacterial pathogenesis, especially in human hosts, it is now

becoming recognized that many pathogens interact with other microorganisms whichmay influence the disease process (11-13).

77 Plant microbial diseases are however still very much considered as being caused by 78 single pure pathogens; nevertheless evidence is also beginning to grow that there can be 79 synergisms between different microorganisms. Recently, a clear example of such 80 synergism has been reported in the olive-knot disease of olive trees (Olea europea L.) 81 caused by the bacterium Pseudomonas savastanoi pv. savastanoi (PSV) (14, 15). PSV 82 possesses a typical LuxI/R AHL QS system and it is involved in virulence since mutants 83 in this system result in significantly smaller knots (15). The bacterial load of the knots 84 (also called tumors) is 50% composed of PSV but also contain a significant proportion of 85 an apparently harmless commensal multispecies bacterial community (16) and some 86 members have been shown to cooperate with PSV resulting in an increase of disease 87 severity (15). More precisely, an Erwinia toletana (ET) strain (harmless to the olive 88 plant) isolated from the olive knot increased disease severity (larger olive-knot) when co-89 inoculated with PSV. In addition, it was demonstrated that ET, Pantoea agglomerans and 90 PSV form stable multispecies communities and that they share and communicate via 91 AHLs. Interestingly, ET and PSV synthesize structurally identical AHLs and co-92 inoculation experiments have evidenced that E. toletana can rescue AHL negative 93 mutants of PSV and restore virulence (15). Microscopy studies have also revealed that 94 ET and PSV co-localize in the olive-knot further indicating that the two species are 95 sharing the same niche both benefiting from this stable interaction. In addition, in silico 96 recreation of the biochemical metabolic pathways encoded by PSV and ET genomes 97 suggested that metabolic complementarity and/or sharing of metabolites could be

98	involved in the beneficial interaction established between these two bacterial species (16).
99	In this work we have further studied the AHL QS systems of PSV and ET, both in vitro
100	and in planta, in order to identify specific molecular determinants involved in this
101	interspecies bacterial interaction. Determination of the PSV and ET QS regulon allowed
102	the identification of several QS-regulated genes putatively involved in numerous
103	metabolic pathways, including the ET aldolase-encoding gene garL, which resulted to be
104	essential for both co-localization of PSV and ET cells inside olive knots and full knot
105	development.

106

107

108

### 109 **RESULTS**

# 110 The luxI/R quorum sensing genes in Pseudomonas savastanoi pv. savastanoi NCPPB

## 111 3335 and Erwinia toletana DAPP-PG 735

112 The olive knot pathogen Pseudomonas savastanoi pv. savastanoi (PSV) NCPPB 3335 113 (17, 18) was the first PSV genome sequenced and has been used in several studies of 114 virulence mechanisms (19). This genome harbors a canonical luxI/luxR pair identical to 115 the previously reported pssI/R QS system of PSV DAPP-PG 722 [hereafter named 116 *pssI/pssR*; (15)] and two *luxR* solos which do not have a cognate *luxI* partner (Figure 1A). 117 From the primary structure of the two LuxR solos, one likely responds to plant signals 118 (designated as LuxR2) and the other most likely to AHLs (designated as LuxR3) (20, 21). 119 Interestingly, this content of LuxI/R QS elements is conserved in all P. savastanoi strains 120 infecting woody plants whose genomes have been sequenced (22-25).

With respect to the olive knot resident and PSV cooperator *E. toletana* (ET), we previously reported that ET DAPP-PG 735 was able to synthesize AHLs via the EtoI/R QS system. The *etoI* mutant, hereafter ETETOI, resulted in no AHL production hence it was concluded that ET possessed one AHL QS system (15). Sequencing of the ET genome (26) and its analysis performed here, surprisingly revealed that ET possessed a second complete canonical AHL QS system. The AHL-responsive transcriptional regulator gene was designated as *tolR* and the autoinducer synthase as *toll* (Figure 1B).

AHL production by *Pseudomonas savastanoi* pv. savastanoi NCPPB 3335 and
 *Erwinia toletana* DAPP-PG 735

QS and AHL production by PSV NCPPB 3335 has not been addressed so far, thus a *pssI*mutant and its complemented strain, expressing the *pssI* gene from a plasmid, were

132 constructed. PSV NCPPB 3335, the pssI mutant and its complemented strain were grown 133 overnight in LB broth and AHLs were extracted from spent supernatants as described in 134 the materials and methods section. C6-AHL production was observed and determined for 135 PSV NCPPB 3335, whereas no AHL production was detected for the  $\Delta pssI$  mutant strain 136 (Table 4 and S1). Interestingly, four types of AHLs (C6-, C8-, 3-oxo-C6- and 3-oxo-C8-137 AHLs) were identified in the supernatant of the  $\Delta pssI$  complemented strain, indicating 138 that overexpression of *pssI* leads to the production of some types of AHLs not detected in 139 the wild type.

140 We also analyzed AHL production by the EtoI/EtoR and ToII/ToIR ET DAPP-PG 735 QS systems. Production of six types of AHL was detected for the wild type ET DAPPG-141 142 PG 735: 3-oxo-C6-, 3-oxo-C8-, 3-oxo-C10-, C6-, C8- and 3-OH-C6-AHLs (Table 4 and 143 S1). We previously reported that this ET strain produced 3-oxo-C6- and 3-oxo-C8-AHLs 144 [15], thus this analytical chemical analysis revealed a wider spectrum of AHL production. 145 As expected, the ETETOI mutant was unable to produce any type of AHL, while the 146 ETETOI complemented strain restored the biosynthesis of all types of AHLs (Table 4 147 and S1). The ETTOLI showed a defect in the biosynthesis of 3-oxo-C10-AHL and 148 unexpectedly it was not restored via the expression of *toll* in trans. The summary of the 149 complete AHL analysis in relation to the peak areas of the detected chromatographic 150 peaks are provided in Table S1 and Figure S3.

151 Transcriptional analysis of quorum sensing genes in PSV NCPPB 3335 and ET
152 DAPP-PG 735

We previously observed that a *pssR* mutant of PSV DAPP-PG 722 produced an amount of AHLs similar to the wild type strain, suggesting that the positive feedback loop typical

155 of AHL QS systems does not occur in PSV. To address this possibility in PSV NCPPB 156 3335, the pssI promoter region was cloned in a promoter probe vector (pMP220) 157 upstream a promoterless lacZ gene and  $\beta$ -galactosidase activity was measured in PSV 158 NCPPB 3335 and its derivative *pssI* and *pssR* mutants during their growth. As shown in 159 Figure 2A, the activity of *pssI* promoter was significantly increased in the stationary 160 phase (10 hours incubation) compared to the exponential phase (4 hours incubation) in all 161 three PSV genetic backgrounds. Moreover, no differences in  $\beta$ -galactosidase activity was 162 observed among the three strains in neither log phase nor stationary phase, thus 163 confirming that the typical AHL QS positive feedback loop does not occur in PSV 164 NCPPB 3335.

165 It was also of interest to study the expression of the ET QS systems; gene promoters of 166 etoI, etoR, tolI and tolR were fused to a promoterless gfp to perform a comparative in 167 vitro transcriptional analysis of both systems in ET, ETETOI and ETTOLI genetic 168 backgrounds. Results showed that toll and tolR genes had considerably lower promoters 169 activities in ET compared to the *etoI* and *etoR* promoters (Figure 2B). Additionally, 170 transcription of *etoR* in ETTOLI was enhanced compared to ET and ETETOI, suggesting 171 that the Toll/TolR system might repress *etoR* transcription. Taking into account the low 172 activity of *toll/tolR* promoters under the *in vitro* conditions used, we questioned if this 173 system was activated in planta. To examine this possibility, co-inoculation of PSV with 174 ET wild type harboring toll promoter fused to GFP were carried out in micropropagated 175 olive plants. No GFP fluorescence was detected for toll promoter, whereas it was 176 observed in the *etoI* promoter fusion, thus demonstrating that *tolI* gene expression was 177 very low also in planta. We then decided to perform a comparative analysis by RT-qPCR

AEM

178 of the transcription of toll and tolR genes in two different media: the King's B rich 179 medium and the Hrp-inducing medium which mimics the plant apoplast (27). Results of 180 this experiment revealed a repression of both genes in the Hrp-inducing medium 181 compared to King's B (Figure S1), which suggests that the environment of the plant 182 might repress toll and tolR transcription. It was therefore concluded that the Toll/R 183 system was functional however it was repressed and/or not activated in ET under 184 laboratory and *in planta* conditions that we have used. It cannot also be excluded that this 185 AHL QS system is functional at very low AHL concentrations.

## 186 Identification of the PSV NCPPB 3335 quorum sensing regulon

187 It was of interest to establish the loci regulated by the PssI/R system thus a whole-188 genome transcriptional RNAseq comparative analysis of wild type PSV NCPPB 3335 189 and its derivative pssI mutant was performed. RNA was extracted from these strains 190 grown in biological triplicates in LB broth to late-log phase and then sequenced as 191 described in Material and Methods section. The results yielded a surprisingly small 192 number of differentially expressed genes (DEGs) between the two strains (Table 5). To 193 evaluate the reliability of the RNAseq results, the expression of these genes was analysed 194 by RT-qPCR. Significant upregulation in the  $\Delta pssI$  mutant was found only for three 195 genes which encoded for PssR (PSA3335\_1621), a pyruvate dehydrogenase E1 196 component beta subunit (PSA3335 1622, pdhT) and a pyruvate dehydrogenase E1 197 component (PSA3335\_1624, pdhQ) (Table 5). On the other hand, downregulation of any 198 of the genes identified by RNAseq analysis was not observed by RT-qPCR (Table 5). In 199 conclusion, after combination of the results obtained by RNAseq and RT-qPCR, the pssI 200 regulon of PSV NCPPB 3335 was restricted to only three genes (pssR, pdhT and pdhQ)

201 under the conditions tested. The pdhT and pdhQ genes were also reported to be under the 202 control of the *pssR* homolog in *P. syringae* pv. *syringae* (PSS) strain B728a (28). 203 Interestingly, in PSS, a regulon study also resulted in very small number of genes 204 regulated by AHL QS which are the same loci also determined to be regulated in PSV in 205 this study (28).

## 206 Identification of the ET DAPP-PG 735 quorum sensing regulon

It was also of interest to determine the AHL QS regulon in ET therefore transcriptional profiling was also performed via RNAseq comparing the wild type against the ETETOI mutant as described in the Materials and Methods section. DEGs of significance ( $p \le$ 0.05) were selected and listed in Table S2. In total, 308 DEGs were identified in the AHL synthase mutant ETETOI mutant, among which 162 loci were down-regulated and 146 up-regulated.

213 Interestingly, 19% of DEGs (59 genes) were classified as carbohydrate metabolism 214 (Table 6) and, among them, 18 loci of inositol catabolism, which were negatively 215 regulated by EtoI/R. On the other hand, DEGs involved in D-galactarate, D-glucarate and 216 D-glycerate catabolism as well as maltose and maltodextrin utilization were positively 217 regulated by the EtoI/R system. Besides carbohydrate metabolism, EtoI/R regulated 218 genes mostly involved in the metabolism of amino acids, loci involved in membrane 219 transport and in respiration. Furthermore, it was established that menaquinone and 220 phylloquinone biosynthesis, glycerolipid and glycerophospholipid metabolism were 221 influenced by EtoI/R. In addition, 9 transcriptional regulators belonging to the DeoR, 222 IclR, LacI and TetR families were regulated by EtoI/R QS system.

Applied and Environmental Microbioloay

In order to corroborate RNAseq results, nine QS-regulated genes were randomly selected and RT-qPCR was carried out with gene-specific primers (Table 3). RNA samples extracted from three biological replicate sets were used as templates for RT-qPCR. Expression patterns determined from RT-qPCR were in good accordance with the expression levels obtained by RNAseq (Figure 3).

## 228 Role of PssI/R of PSV NCPPB 3335 in planta

In order to determine the role of the AHL QS system of PSV NCPPB 335 in virulence, the  $\Delta pssI$  and  $\Delta pssR$  mutants and their respective complemented strains were inoculated in micropropagated and in woody olive plants. In our conditions, no significant differences in knot development among the strains tested were found either in non-woody (micropropagated) or woody olive plants (Figure 3). Additionally, all bacteria reached a similar final population within the knots. It was concluded that PSV NCPPB 3335 AHL QS did not play a significant role in virulence under the conditions tested.

236 In planta role of QS regulated loci of ET

In order to study the possible role of some ET AHL QS regulated loci in the cooperative
interaction with PSV, knock-out mutants in *iolD*, *iotS*, *garL*, *malK*, *gldA* and *hslV* genes
were generated by insertion mutagenesis and co-inoculated with PSV in olive plants.
Four of these DEGs (*iolD*, *iotS*, *garL* and *malK*) are involved in carbohydrate metabolism,
which is the most representative category regulated by AHL QS in ET (see above). The *gldA* and *hslV*, on the other hand, encode for a glycerol dehydrogenase and ATPdependent protease.

As previously established, co-inoculation of PSV with ET significantly increased the size of the olive knot (15, 16). When ET mutants, ETIOTS, ETMALK, ETGLDA and

246	ETHSLV were co-inoculated with PSV, olive knot size did not show any significant size
247	alteration when compared when co-inoculated with ET wildtype (Figure 4A). Co-
248	inoculation of PSV with ETGARL and ETIOLD, on the other hand, had a significant
249	effect on the olive knot size with approximately a 50% reduction for ETGARL and
250	approximately 20% increase for ETIOLD (Figure 4A). When co-inoculated with
251	ETGARL, the colony forming units (CFU) of PSV in the knot were significantly reduced
252	and resulted in 20% the amount of cells when co-inoculation was performed with the
253	wildtype ET (Figure 4B). A significant reduction in the CFUs of PSV was also observed
254	when co-inoculated with ETIOTS, ETGLDA and ETHSLV regardless that olive-knot
255	size was not significantly affected. In order to further determine the putative role of GarL
256	in PSV-ET interaction, we co-inoculated GFP-labeled PSV with ET wild type or the garL
257	mutant constitutively expressing RFP. At 30 dpi knots were visualized in a stereoscopic
258	microscope using GFP and RFP filters (Figure 5A, 5B) and pictures were taken and
259	processed as described in Materials and Methods. Results show that the percentage of
260	PSV population co-localization with ET wild type is under 5%, whereas over 75% of ET
261	co-localize with PSV (Figure 5C). On the other hand, mutation in the ET garL gene
262	resulted in a drastic reduction of ET association with PSV, with only 6.6% of the total ET
263	population overlapping PSV. This result, together with the reduced knot size in PSV-
264	ETGARL co-inoculation, indicated that GarL plays a major role in PSV-ET interaction.

### 265 DISCUSSION

266 There is a growing need to study interspecies bacterial interactions since it is now 267 becoming evident that most bacteria in the wild live as part of complex communities. 268 Moreover in relation to diseases, reports are beginning to demonstrate that pathogens 269 undergo interactions and communicate with non-pathogenic commensal/resident host 270 microbial flora (11, 29). We have previously reported that the olive knot disease is a 271 model to study interspecies communication and cooperation between a bacterial pathogen 272 and commensal bacteria in a plant disease (14, 15). This cross-communication occurs via 273 cross-feeding/sharing of AHL QS signals whereas the mechanism(s) of cooperation 274 leading to a more aggressive disease is currently not understood and could be due to 275 metabolite(s) sharing and/or metabolic complementarity. In this study, we determined the 276 QS regulons of PSV and ET in order to begin to shed some light in this cooperative 277 interspecies interaction in a plant disease.

278 Results presented here reveal that all P. savastanoi isolates infecting woody plants 279 sequenced so far, harbor an identical content of AHL QS-related genes which consist of 280 an archetypical AHL QS pair designated as *pssl/pssR*, and two *luxR* solos. The Pssl/R 281 system was firstly reported in strain DAPP-PG 722 (15) and displays 100% identity with 282 PssI/R of strain NCPPB 3335 (studied here). At transcriptional level there is no QS 283 positive feedback loop regulating the AHL synthase gene in PSV NCPPB 3335 (Figure 284 2A), which is contrast with what occurs in *P. syringae* pv syringae (PSS) B728a [50], a 285 strain closely related with PSV from a phylogenetic point of view. It cannot be excluded 286 that one of the two LuxR solos present in PSV genomes might be involved in pssI 287 regulation. Moreover, AefR (<u>AHL epiphytic fitness Regulator</u>) positively regulates the

*pssI* homolog *ahlI*, in *P. syringae* pv *phaseolicola* NPS3121 (30) and PSS B728a (31); a
homolog of AefR is present in PSV genomes and could therefore have a similar function
in regulating *pssI* in PSV.

*In planta* infection studies revealed that in PSV NCPPB 3335 neither *pssI* nor *pssR* are involved in virulence in the olive plant. It cannot be excluded however that AHL QS in PSV might plays a role in the epiphytic fitness/lifestyle *in planta*; QS has been shown to play a role in epiphytic fitness in PSS as well as other plant-associated bacteria (28, 31-33).

296 We found that wild type PSV NCPPB 3335 produces exclusively C6-AHL, whereas PSV 297 DAPP-PG 722 synthesizes 3-oxo-C6- and 3-oxo-C8-AHLs (15) regardless that the luxI 298 homologs are 100% identical; some other factor(s) might be responsible for the 299 generation of different signal molecules. Overexpression of pssI in PSV NCPPB 3335 300 yielded 3-oxo-C6- and 3-oxo-C8-HSLs in addition to C6-AHL (Table 2), suggesting that 301 different expression levels between these two strains might explain differences in AHL 302 production. AHLs are synthesized by LuxI using S-adenosylmethionine and an acyl 303 group which is provided by an acyl-carrier protein (ACP) (34). We have identified an 304 ACP-encoding gene in the genome of PSV DAPP-PG 722 (locus tag GS14\_RS0122650) 305 which is not present in the PSV NCBBP 3335 genome; this locus might be involved in 306 AHL synthesis and consequently lead to a dissimilar AHL profile synthesis between 307 these two PSV strains. We previously reported 3-oxo-C6- and 3-oxo-C8-AHL production 308 by ET DAPP-PG 735 (15) and here we demonstrated the production of four additional 309 types of AHL (C6-, C8-, 3-oxo-C10- and 3-OH-C6-AHLs) using a more sensitive 310 technique. The ability to produce more AHL types by ET increases its ability to crosstalk with bacterial neighbours. The PSV NCPPB 3335 can synthesize three out of the six
types of AHL produced by ET indicating possible eavesdropping between PSV and ET
via these AHLs. This is in line with our previous study which demonstrated rescue of the
PSV QS response of a *pssI* mutant by co-inoculation with ET wild type (15).

315 This study reports the genetic loci regulated by AHL QS in a woody host pathogen of the 316 P. syringae complex. Previous reports involve the two P. syringae herbaceous pathogens 317 P. syringae pv syringae (PSS) and P. syringae pv. tabaci (PST). PSV NCPPB 3335 318 AHL QS regulon consists of only three genetically close loci, namely pdhT, pdhQ and 319 pssR. In PSS strain B728a AHL QS regulates the transcription of only a 9 gene cluster 320 located adjacent to the *ahlR-ahll* locus which also contains the *pdhT* and *pdhQ* loci (28), 321 whereas in PST strain 11528 over 300 genes were found to be regulated by QS, 322 including phdT, pdhQ and the *pssR* homologs (35). Despite such a difference in AHL QS 323 regulons among these strains, the transcription of pdhT, pdhQ and pssR (ahlR) is 324 common in all P. syringae species and their role in P. syringae deserves further attention. 325 (36).

326 QS in *Erwinia* species plays important roles in virulence determinants and secondary 327 metabolite production (37). E. toletana is a harmless epiphyte and endophyte and was 328 first isolated from olive knots caused by PSV, and is now a model to study multispecies 329 interactions with PSV (14). ET DAPP-PG 735 possesses two canonical AHL QS systems, 330 designated as EtoI/R and ToII/R. Prior to the availability of the genome sequence, AHL 331 QS signals produced by ET were initially only attributed to EtoI (15). Here we report that 332 promoter activities of *toll/R* in ET, ETTOLI and ETETOI were very low and were barely 333 detectable in planta and were found to be repressed by the plant apoplast mimic medium,

15

Applied and Environmental

AEM

<u>Applied</u> and Environmental

Microbiology

334

335

336

337

338

339

repressed.

340 In ET, 308 genes were found to be regulated by EtoI/R controlling diverse functions such 341 as membrane transport, protein metabolism, respiration, stress response, cell division and 342 cell cycle. Interestingly, 59 loci were involved in metabolism of carbohydrates including 343 inositol, D-galactarate, D-glucarate, maltose and maltodextrin indicating that it plays an 344 important role in carbon resource acquisition. It was therefore of interest to study whether 345 any of these carbohydrate metabolic pathways play a role in interspecies interactions and 346 cooperation with PSV. As shown in Figure 4, when co-inoculated with several ET 347 mutants in these pathways, PSV reached lower population densities, indicating that *iotS*, 348 garL, gldA and gslV ET genes play a role in PSV-ET cross-communication. IN addition, 349 co-inoculation of the ET garL mutant with PSV resulted in a significantly smaller olive 350 knot. The alpha-dehydro-beta-deoxy-D-glucarate aldolase GarL catalyzes the cleavage of 351 both 5-keto-4-deoxy-D-glucarate and 2-keto-3-deoxy-D-glucarate to pyruvate and 352 tartronic semialdehyde (44). GarL is involved in D-galactarate, D-glucarate and D-353 glycerate catabolism synthesizing D-glycerate from galactarate. This demonstrates that 354 ET-PSV cross-communication also occurs through some reactions of primary metabolism 355 that not only affect the growth of PSV in planta, but also its virulence.

suggesting that *toll/R* is stringently regulated and might need a yet unidentified stimulus

to be expressed. It is common that two or more AHL QS systems coexist in one

bacterium and many of these are interconnected in their regulation (38-43). The

uniqueness in *E. toletana* is that one system is stringently regulated probably requiring, in

addition to cell-density, an environmental stimulus in order to be activated and/or de-

In summary, this work further demonstrated the role of AHL QS in the olive knot as well
as metabolic interaction. This therefore further highlights the olive knot as a good model
to study bacterial interspecies interactions in planta of a plant disease.

359

17

Applied and Environmental Microbiology

AEM

Applied and Environmental Microbiology

### 360 MATERIALS AND METHODS

## 361 Bacterial strains, media, growth conditions and recombinant DNA techniques

Bacterial strains used in this study are listed in Table 1. PSV and ET were grown at 28 °C and *Escherichia coli* was grown at 37 °C in Luria-Bertani (LB) medium (45) and Super Optimal Broth (SOB) (46). Solid and liquid media were amended when required with the appropriate antibiotic. Antibiotic concentration used were: kanamycin (Km) 10  $\mu$ g ml<sup>-1</sup> for PSV and 50  $\mu$ g ml<sup>-1</sup> for *E. coli*, gentamycin (Gm) 10  $\mu$ g ml<sup>-1</sup>, ampicillin (Ap) 400  $\mu$ g ml<sup>-1</sup> for PSV and 100  $\mu$ g ml<sup>-1</sup> for *E. coli*; and tetracycline 10  $\mu$ g ml<sup>-1</sup>.

All recombinant DNA techniques including restriction digestion, and agarose gel electrophoresis, purification of DNA fragments and ligations with T4 DNA ligase were performed as previously described (47). Plasmids were purified by using EuroGold columns (EuroClone, Italy) and were sequenced by Macrogen Europe (Amsterdam, NL) when necessary.

### 373 Construction of bacterial strains

374 Plasmids and oligonucleotides used in this study are listed in Tables 2 and 3, respectively. 375 PSV NCPPB 3335 pssI (PSA3335\_1620) and pssR (PSA3335\_1621) mutants were 376 generated by allelic interchange. DNA fragments of approximately 1 kb corresponding to 377 the upstream and downstream flanking regions of the gene to be deleted were amplified 378 in three rounds of polymerase chain reaction (PCR) using Expand High Fidelity 379 polymerase (Roche Applied Science, Mannheim, Germany). Restriction sites for HindIII 380 were included in the primers as previously described (48). The resulting products, 381 consisting on upstream and downstream flanking regions separated by the HindIII 382 restriction site, were cloned into pGEMT-Easy (Promega, Madison, WI, U.S.A.) and

387	Plasmids were transferred to NCPPB 3335 by electroporation (17) and transformants
388	were selected in LB-Km plates. To select the allelic interchange (double recombination
389	event) and discard plasmid integration (single recombination event), individual colonies
390	were replicated into LB-Ap plates and Ap <sup>R</sup> colonies were discarded. Southern blot
391	analyses were carried out to confirm single integration in the correct position in PSV
392	genome.
393	Mutation of selected genes in ET was performed via a single homologous recombination
394	event with the use of pKNOCK-Km suicide delivery system as previously described (50)
395	generating mutants of ETIOLD, ETIOTS, ETGARL, ETMALK, ETGLDA, ETHSLV,

sequenced to discard mutations. Next, the kanamycin resistance gene nptII was extracted

by enzyme restriction from pGEMT-KmFRT- HindIII (49) and cloned in the plasmids

mentioned above to generate pECP10-Km and pECP11-Km (Table 2). All the plasmids

generated for the construction of PSV NCPPB 3335 mutants were suicide vectors in PSV.

39 396 ETTOLI and ETTOLR. Briefly, internal fragments from iolD (G200 RS0103425), iotS 397 (G200\_RS0119945), garL (G200\_RS0124305), malK (G200\_RS0114460), gldA 398 (G200\_RS0114990), hslV (G200\_RS0113655), tolI (G200\_RS0118785) and tolR 399 (G200\_RS0118780) of ET were amplified using the primers listed in Table 3 and cloned 400 in conjugative suicide vector pKNOCK-Km. The generated plasmids having internal 401 fragments from selected genes were transformed into E. coli S17-1 Apir and delivered to ET for its homologous recombination. Km<sup>R</sup> colonies were verified by PCR analysis 402 403 followed by sequencing of the targeted gene to confirm the generation of ET mutants.

#### 404 AHL extraction and characterization

AEN

Applied and Environmental

Microbioloav

405 Bacterial strains were grown overnight in LB broth (final volume 100 ml); cells were 406 then removed by centrifugation and the supernatant was used to purify AHLs. Spent 407 supernatants were filtered (pore diameter 0.45  $\mu$ m), mixed with one volume of 0.1% 408 acetic acid (v/v) in ethyl acetate and incubated under shaking conditions for 30 minutes. 409 The organic phases were dried at room temperature. The AHLs produced by each strain 410 were identified from the organic extracts of spent supernatants by liquid chromatography-411 electrospray ionization-tandem mass spectrometry (LC-ESI-MS/MS) as we described 412 previously (51). As an example of this analysis, the ion chromatograms of an AHL 413 standard and the *E. toletana* wild type sample is provided in Figure S3.

## 414 Construction of plasmids and reporter assays

For the complementation of PSV  $\Delta pssI$  and  $\Delta pssR$  mutant strains, the entire open reading frames of each gene and their corresponding promoter and transcriptional terminator regions were amplified by PCR using Expand High Fidelity polymerase (Roche Applied Science, Mannheim, Germany) and cloned into pGEMT-Easy (Promega, Madison, WI, USA). After sequencing to discard mutations, the fragments were directionally subcloned into pBBR:MCS5 yielding pBBR:*pssI* and pBBR:*pssR*.

421 DNA fragments of 338 and 352 bp containing *pssI* and *pssR* promoter regions, 422 respectively, were amplified by PCR using oligonucleotides listed in Table 3 and cloned 423 into pMP220 (52). The resulting plasmid *lacZ* transcriptional fusions were transferred to 424 PSV by electroporation and  $\beta$ -galactosidase activity was measured as described 425 previously (45). Bacteria were grown in LB broth amended with 10 µg ml<sup>-1</sup> tetracycline 426 at an initial OD<sub>600nm</sub> of 0.3 and  $\beta$ -galactosidase activity was measured throughout the 427 growth curve. 428 Promoter regions of etoI, etoR, tolI and tolR ET genes were amplified by PCR using the 429 oligonucleotides listed in Table 3 and cloned in the vector pBBR:GFP (53) in order to be 430 transcriptionally fused to a promoterless gfp gene. The resulting plasmids were 431 transformed by electroporation into ET strains (54) and gene promoter activity was 432 determined as the amount of GFP fluorescence measured in the late log phase at 510nm 433 on a microplate reader (Perkin Elmer EnVision 2104). The expression of toll and tolR 434 was also analyzed by RT-qPCR in King's B and Hrp-inducing medium as reported 435 previously (48). The etoI and toll promoter activities were measured in vivo in mixed 436 PSV-ET infections. Ten plants were inoculated with each of the three combinations: PSV 437 and ET expressing a promoterless GFP (negative control), PSV and ET-pBBR:P<sub>etol</sub>-GFP, 438 and PSV and ET-pBBR:Ptoll-GFP. The presence/absence of fluorescence was verified 439 using a stereoscopic microscope (Leica MZ FLIII; Leica Microsystems, Wetzlar, 440 Germany).

## 441 RNA extraction, RNAseq and analysis

442 Ribopure bacteria RNA isolation kit (Ambion Inc., Austin, TX, U.S.A.) was used for 443 total RNA extraction from three biological replications. Bacteria were grown in LB until the onset of stationary phase and about 2 x 10<sup>9</sup> cells were collected for RNA extraction 444 445 following the manufacturer's instructions. Library preparation and transcriptome 446 sequencing were performed by IGA Technology Services Srl (Udine, Italy). Briefly, 447 libraries were constructed with TruSeq Stranded mRNA Sample Prep kit (Illumina, San 448 Diego, CA) and single-end sequencing was carried out on HiSeq2500 (Illumina, San 449 Diego, CA). Illumina adapters, lower quality bases and poly-A tails were removed using 450 ERNE (55). Software and tools for *de novo* assembly and comparisons were performed as

451 previously described (56-58). The false discovery rate (FDR) with a significance level of 452  $\leq 0.05$  and with a minimum fold change set as the threshold were used to judge the 453 significance of gene expression difference. Reads obtained from adapter removal were 454 aligned against GCA 000336255.1 and GCA 000164015.2 reference genome assemblies. 455 Features counts produced by RNA-seq were normalized and analyzed with DeSeq2 456 software (http://dx.doi.org/10.1186/s13059-014-0550-8) to calculate differential 457 expression values ( $\log_2$  of the fold change LFC) and raw p-values. To select differentially 458 expressed genes, genes raw p-values were corrected for multiple testing using with the 459 false discovery rate (FDR) method (59). Final selection was based on genes with FDR 460  $\leq 0.05$ . The original RNAseq data has been submitted in the Sequence Read Archive 461 (SRA) as submission number SUB3743389

## 462 Validation of RNAseq data using qRT-PCR

463 Quantitative real-time PCR was performed on CFX96 Touch qPCR system (Bio-Rad, 464 Hercules, CA, USA) to validate expression patterns from transcriptome analysis. cDNA 465 was generated following the manufacturer's protocol of Reverse Transcription system kit 466 (Promega, Madison, WI, USA) starting with 1-2 µg of purified RNA as input. Diluted with RNase-free water, the synthesized cDNA samples were adjusted to 25 ng  $\mu$ L<sup>-1</sup> and 467 468 were measured by Nano Drop 2000 (Thermo scientific, Wilmington, DA, USA). In each 469 reaction, 2 µL of cDNA template was mixed with GoTaq qPCR Master Mix kit (Promega, 470 Madison, WI, USA) and specific primers (Table 3) to a final volume of 12  $\mu$ l. qPCR 471 primer designing was performed with free online software following the instructions of 472 Brenda Thornton and Chandak Basu (60). Each reaction was carried out initially with 2 min at 95 °C, followed by 45 cycles of PCR (95 °C, 15 s; 60 °C, 30 s). The relative 473

Accepted Manuscript Posted Online

Applied and Environmental

AEM

474 transcript abundance was calculated using the cycle threshold ( $\Delta\Delta$ Ct) method (61). 475 Transcriptional data were normalized to the gyrA (for PSV) or recA (for ET) 476 housekeeping genes.

#### 477 In planta experiments

478 Olive plants were micropropagated and inoculated as detailed previously (62). Briefly, 479 micropropagated olive plants were wounded by excision of an intermediate leaf and 480 infected in the stem wound with a bacterial suspension under sterile conditions. For this 481 purpose, bacterial lawns were grown for 48h on LB plates, washed twice with 10 mM 482  $MgCl_2$  and resuspended in 10 mM  $MgCl_2$  to an approximate concentration of  $10^8$ CFU·mL<sup>-1</sup>. Suspension of PSV alone or mixed with ETIOLD, ETIOTS, ETGARL, 483 484 ETMALK, ETGLDA and ETHSLV respectively in 1:1 (vol:vol) ratio were prepared. Plants were inoculated with approximately  $5 \times 10^3$  total CFU and kept in a growth chamber 485 486 for 30 days, as previously described (62). The morphology of the knots was observed 487 with a stereoscopic microscope 30 days post-inoculation (dpi) (Leica MZ FLIII; Leica 488 Microsystems, Wetzlar, Germany), also equipped with a 100 W mercury lamp, a GFP2 489 filter (excitation 480/40 nm; emission 510LP nm) and a red fluorescent protein (RFP) 490 filter (excitation 546/10 nm; emission 570LP nm). For the quantification of green (GFP-491 tagged PSV) and red (RFP-tagged ET and ETGARL strains) pixels, two pictures per knot 492 (corresponding to the front and back sides of the tumour) were taken with each the GFP2 493 and RFP filters. Pictures were transformed to 8-bits images and overlapped with Fiji 494 ImageJ (https://imagej.net/Fiji) using the Image correlator plugin. The number of green 495 pixels overlapping red pixels, indicating the population of PSV that co-localize with 496 ET/ETGARL, was determined for both the front and the back sides of each knot and an

497	average per knot was calculated. An identical procedure was used to determine the
498	percentage of ET or ETGARL population that co-localize with PSV. Bacteria were
499	recovered from the knots using a mortar and pestle containing sterile $MgCl_2$ 10 mM.
500	Serial dilutions were plated on LB plates supplemented with the corresponding antibiotic
501	when required. Knots were 3D scanned and the knot size determined using the Neftabb
502	Basic 5.2 software.

503 The virulence of PSV and its derived mutants and complemented strains was also 504 analysed on 1-year old olive plants on 1-year old olive plants (Olea europaea) derived 505 from a seed originally collected from a cv. Arbequina plant as detailed before (17, 63, 64). 506 Morphological changes scored at 90 dpi were captured with a high-resolution camera 507 Canon D6200 (Canon Corporation, Tokyo, Japan). The knot volume was calculated from 508 a minimum of three representative knots as described previously (15, 65).

509

#### 510 Acknowledgements

511 ECP acknowledges the contribution of an EMBO fellowship, MX of a Chinese 512 Scholarship Council fellowship whereas DPD and GU of an ICGEB fellowship.

513

514

Applied and Environmental

Microbiology

## 515 Figure Legends

516	Figure 1. Gene arrangement of quorum sensing system elements in the genomes of PSV
517	NCPPB 3335 and ET DAPP-PG 735. (A) pssI and pssR represent a canonical luxI/luxR
518	gene pair, whereas <i>luxR2</i> and <i>luxR3</i> correspond to orphan <i>luxR</i> homologs in PSV NCPPB
519	3335. (B) <i>etol/etoR</i> and <i>toll/tolR</i> represent two canonical <i>luxl/luxR</i> gene pairs of ET
520	DAPP-PG 735. Codes above arrows correspond to locus tags
521	Figure 2. Promoter activities of PSV and ET quorum sensing genes. (A) $\beta$ -galactosidase
522	activity of <i>pssI</i> promoter fusion to <i>lacZ</i> measured in PSV NCPPB 3335, $\Delta pssI$ and $\Delta pssR$
523	at log (4 hours incubation) and stationary phase (10 hours incubation). PSV harboring a
524	promoterless lacZ (empty pMP220 plasmid) was included as a control. Asterisks indicate
525	a significant difference (student's t test, $P < 0.05$ ) in promoter activity in stationary phase
526	compared to log phase (B) GFP fluorescence of etoI, etoR tolI and tolR fusions to gfp
527	measured in ET, ETTOLI and ETETOI backgrounds. GFP fluorescence was normalized
528	to $OD_{600}$ . Bars represent the average of three independent replications $\pm$ the standard
529	deviation
530	Figure 3. Evaluation of RNAseq-based expression patterns of ET using RT-qPCR. The
531	expression patterns of randomly selected genes were analyzed by RT-qPCR to validate
532	RNAseq results. The values of fold difference were average of three biological replicates
533	which were calculated by using comparative quantification method. $Log_2$ ratio of
534	obtained values was compared with log <sub>2</sub> ratio of (ETETOI/ET) FPKM values.
535	Figure 4. Role of ET AHL QS loci in the PSV-ET cooperation in planta. (A) Size of the
536	knots induced in micropropagated olive plants at 30 dpi by PSV in combination with ET

- 537 strains. (B) CFU of PSV and (C) CFU of ET recovered from knots. Bars indicate the
- 538 average of, at least, three knots  $\pm$  standard deviation.
- 539 Figure 5. Knots developed at 30 dpi in micropropagated olive plants after co-inoculation
- 540 of GFP-labelled PSV with RFP-labelled ET or ETGARL. (A) Co-inoculation using GFP-
- 541 labelled PSV and RFP-labelled ET. (B) Co-inoculation using GFP-labelled PSV and
- 542 RFP-labelled ETGARL. (C) Percentage of the PSV and ET/ETGARL populations co-
- 543 localization within the knot. Bars represent the average of six independent knots  $\pm$
- 544 standard deviation.

545

- 546
- 547
- 548 549
- 550
- 551
- 552

Applied and Environmental

Microbiology

# 553 554 Table 1. Bacterial strains used in this study

Bacterial Strains	Relevant characteristics	Source	
Escherichia coli			
DH5a	$F-\Phi 80 lac Z\Delta M15 \Delta (lac ZYA-argF) U169$	Invitrogen-LifeTechnologies	
	recA1 endA1 hsdR17 (rK-, mK+) phoA		
	supE44 λ– thi-1 gyrA96 relA1		
S17-1λpir	Km <sup>R</sup> , recA, pro, hsdR, RP4-Tc::Mu-Km::Tn7,	(66)	
	pir		
Erwinia toletana			
DAPP-PG 735	Wild type	(15)	
ETETOI	Deletion etoI mutant of ET DAPP-PG735	(15)	
ETETOR	Deletion <i>etoR</i> mutant of ET DAPP-PG735	(15)	
ETTOLI	Deletion toll mutant of ET DAPP-PG735	This study	
ETTOLR	Deletion tolR mutant of ET DAPP-PG735	This study	
ETIOLD	Deletion <i>iolD</i> mutant of ET DAPP-PG735	This study	
ETIOTS	Deletion <i>iotS</i> mutant of ET DAPP-PG735	This study	
ETGARL	Deletion garL mutant of ET DAPP-PG735	This study	
ETMALK	Deletion <i>malK</i> mutant of ET DAPP-PG735	This study	
ETGLDA	Deletion gldA mutant of ET DAPP-PG735	This study	
ETHSLV	Deletion <i>hslV</i> mutant of ET DAPP-PG735	This study	
ETETOI-	ETETOI complemented with pBBR:etoI	This study	
pBBR:etoI			
ETTOLI-pBBR:toll	ETTOLI complemented with pBBR:toll	This study	
Pseudomonas			
savastanoi pv.			
savastanoi			
NCPPB 3335	Wild type	(17)	
$\Delta pssI$	Deletion <i>pssI</i> mutant of NCPPB 3335 (Km <sup>R</sup> )	This study	
$\Delta pssR$	Deletion <i>pssR</i> mutant of NCPPB 3335 (Km <sup>R</sup> )	This study	
ΔpssI-pBBR:pssI	$\Delta pssI$ complemented with pBBR:pssI	This study	
$\Delta pssR$ -pBBR:pssR	$\Delta pssR$ complemented with pBBR:pssR	This study	

555

Applied and Environmental Microbiology

# 556 557 Table 2 Plasmids used in this study

Tuble 2 Thashinds used	in this study	
pGEM-T Easy	Cloning vector; Amp <sup>R</sup>	Promega
pGEM-T Easy pKNOCK-Km	Conjugative suicide vector; Km <sup>R</sup>	(50)
pKNOCK-IOLD	Internal PCR iolD fragment of ET DAPP-PG	This study
pRNOCK-IOLD	735 cloned in pKNOCK-Km; Km <sup>R</sup>	This study
pKNOCK- IOTS	Internal PCR iotS fragment of ET DAPP-PG	This study
pRIVOCK-1015	735 cloned in pKNOCK-Km; Km <sup>R</sup>	This study
pKNOCK- GARL	Internal PCR garL fragment of ET DAPP-PG	This study
philoek onice	735 cloned in pKNOCK-Km; Km <sup>R</sup>	This study
pKNOCK- MALK	Internal PCR malK fragment of ET DAPP-PG	This study
pritoer miller	735 cloned in pKNOCK-Km; Km <sup>R</sup>	This study
pKNOCK- GLDA	Internal PCR gldA fragment of ET DAPP-PG	This study
philoen olbh	735 cloned in pKNOCK-Km; Km <sup>R</sup>	This study
pKNOCK- HSLV	Internal PCR hslV fragment of ET DAPP-PG	This study
pintoon nozt	735 cloned in pKNOCK-Km; Km <sup>R</sup>	inio study
pECP10-Km	pGEM-T Easy derivative containing 1kb on	This study
F	each side of the <i>pssI</i> (PSA3335_1621) gene	
	from NCPPB 3335 interrupted by the	
	kanamycin resistance gene <i>nptII</i> (Ap <sup>R</sup> , Km <sup>R</sup> )	
pECP11-Km	pGEM-T Easy derivative containing 1kb on	This work
*	each side of the <i>pssR</i> (PSA3335 1622) gene	
	from NCPPB 3335 interrupted by the	
	kanamycin resistance gene $nptII$ (Ap <sup>R</sup> , Km <sup>R</sup> )	
pGEMT-KmFRT-HindIII	Contains KmR from pKD4 and HindIII sites	This work
*	(ApR KmR)	
pBBR:pssI	pBBR1MCS-5-derivative containing the PSV	This work
	NCPPB 3335 pssI and its promoter region (352	
	bp) flanked by EcoRI and XbaI restriction sites	
	(Gm <sup>R</sup> )	
pBBR:pssR	pBBR1MCS-5-derivative containing the PSV	This work
	NCPPB 3335 <i>pssR</i> and its promoter region (435	
	bp) flanked by <i>EcoRI</i> and <i>XbaI</i> restriction sites	
	(Gm <sup>R</sup> )	
pMP220	Promoter probe vector, IncP, LacZ; Tc <sup>R</sup>	(52)
pMP220-PpssI	Transcriptional fusion of PSV pssI promoter to	This work
	lacZ	
pLRM1-GFP	Overexpression of GFP from pBBRMCS5	(67)
pBBR:RFP	pBBRMSC5 containing RFP	(53)
pBBR:GFP	pBBRMSC5 containing a promoterless GFP	(53)
pBBR:Petol-GFP	Transcriptional fusion of ET <i>etoI</i> promoter to GFP	This work
		TT1.'
pBBR:PetoR-GFP	Transcriptional fusion of ET <i>etoR</i> promoter to GFP	This work
"DDD.Dtoll CED		This work
pBBR:Ptoll-GFP	Transcriptional fusion of ET <i>toll</i> promoter to GFP	THIS WORK
"PPD.DtolR CED	Transcriptional fusion of ET <i>tolR</i> promoter to	This work
pBBR:PtolR-GFP	GFP	THIS WOLK
pBBR:etoI	pBBR1MSC-5 containing <i>etoI</i> , Described as	(15)
PEDREIOI	pBBRToll in previous publication	(13)
pBBR:toll	pBBR1MSC-5 containing toll	This work
r- Dianon	r	

558 559

# 560 561 Table 3 Primers used for cloning purposes

Primers used for clor	ning purposes				
Plasmid	Primer name Primer sequence				
pKNOCK-IOLD iolD_pnkFw AGATCTCACCAGATTCCGTTTGCCG					
-	iolD_pnkRev	CTCGAGCTGTTGTAATCCCTGGTGCG			
pKNOCK- IOTS	iotS_pnkFw	AGATCTGCTGACCGATAAAATGGCGT			
<b>I</b>	iotS_pnkRev	CTCGAGACCAATCGCCATTTCATCGT			
pKNOCK- GARL	garL_pnkFw	AGATCTGTCCACCTTGCAACGAACC			
r	garL_pnkRev	CTCGAGGAGCTGGGTTTCGATTTGCA			
pKNOCK- MALK	malK_pnkFw	AGATCTATTGGTCGCACGCTGGTC			
pintoon minin	malK_pnkRev	CTCGAGCGATGGCCTTGTTAGTGACC			
pKNOCK- GLDA	gldA_pnkFw	AGATCTCCGATGAAGGGGTGTTTGAA			
philoen oldin	gldA_pnkRev	CTCGAGCCAGACCGCCATTCTCAAAG			
pKNOCK- HSLV	hslV_pnkFw	AGATCTGGTCATCTGGTTAAAGCCGC			
privock-nstv	hslV_pnkRev	CTCGAGCACCTGAACCGATGGCAATA			
pKNOCK-tolI					
PKNOCK-1011	muttolIFw	GGATCACTGTGCCCTTTA			
KNOCK (11)	muttolIRev	TTATCCTCAGAGTGAATCAGCC			
pKNOCK-tolR	muttolRFw	TACGCGACCTGAGACGCATC			
	muttolRRev	ATTTTACGATTTCCAGCTCGCG			
pBBR:Ptoll-GFP	PtolIFw	CAGAGATCTCGCTGATTC			
	PtolIRev	CGAATTCCGCCAACAACGA			
pBBR:PtolR-GFP	PtolRFw	AATCGTGGATCCGCGG			
	PtolRRev	CGAATTCACCACACCAG			
pBBR:PetoI-GFP	PetoIFw	TTAGATCTAAATCACGTAACAAC			
	PetoIRew	ATTCGAATTCATATCAAA			
pBBR:PetoR-GFP	PetoRFw	CAGATCTGCTCTTCCTGTAATGGGA			
	PetoIRew	CGAATTCACATTTGCCTGACCTCAA			
pBBR:pssI	pssI_F-331	TCTAGATCGCTCTGATCCTGATGAGTG			
	pssI_R924	GAATTCCTCATCCGCTTCCATGACC			
pBBR:pssR	pssR-F-417	TCTAGAAGACGCTCGACGATGTCG			
	pssR_R993	GAATTCTTGCAATCGATCATCACGG			
pBBR:toll	tolIFw	GTCTCGAGCAAATCTGCTGATGCCGC			
•	tolIRev	GGACTAGTGCCTGGCTGCTGATTACTTT			
pMP220-PpssI	pssI_F-279	ACTCATGGAGATCTGGCAGAGATTTCGTGTTGGG			
	pssI_R35	ACTCATGGGGTACCGTAACGGGCATCGTCGTG			
pBBR:pssI	pssI_F-331	TCTAGATCGCTCTGATCCTGATGAGTG			
r - r	pssI_R924	GAATTCCTCATCCGCTTCCATGACC			
pBBR:pssR	pssR-F-417	TCTAGAAGACGCTCGACGATGTCG			
rr	pssR_R993	GAATTCTTGCAATCGATCATCACGG			
Primers used for the					
pssR	PssR_F-1008	CATTCCAGTGCTCCTTGAGC			
poor	TAPssR_R3	AAGCTTGACTCACTATAGGGGCTTTCACGGTACGA			
	nn ssic_its	ACCTC			
	TDPssR R739	CCCTATAGTGAGTCAAGCTTCCATCAACATGGGCA			
	101351(_1(15)	GG			
	PssI_F-332	CCTGATGAGTGTGTGCATCG			
pssI	TAPssI_R4	CCCTATAGTGAGTCAAGCTTCATGCATAGCGCTGCC			
<i>p</i> 331	1711 331_1(4	TG			
	PssI F-983	GATATCGGCGTTGATGTCCTG			
		onnieddediffondietero			
		CCCTATAGTGAGTCAAGCCTTCATGCATAGCCCTCCC			
	TDPssI_F680	CCCTATAGTGAGTCAAGCTTCATGCATAGCGCTGCC			
	TDPssI_F680	TG			
Drimors used in the -	TDPssI_F680 PssR_F-280				
Primers used in the q	TDPssI_F680 PssR_F-280 PCR experiments	TG TGCGCTGTTCATCACTACTCC			
Gene ID	TDPssI_F680 PssR_F-280	TG			
Gene ID E. toletana genes	TDPssI_F680 PssR_F-280 PCR experiments Gene function	TG TGCGCTGTTCATCACTACTCC Primer sequence			
Gene ID	TDPssI_F680 PssR_F-280 PCR experiments	TG TGCGCTGTTCATCACTACTCC Primer sequence			

		R: GGCGAACAGAGGCGTAGA
G200_RS0112020	Sigma-fimbria uncharacterized	F: CCTCGGTGTTGCCTCTTC
	paralogous subunit	R: CCATTGCCTGCTGAACCC
G200 RS0112675	SulP family transporter	F:GTGTATGTGGTGGCGGTG
	5	R: CACTGAGGTAATCGGCAAGC
G200 RS0113655	ATP-dependent protease HslV	F: GTAGTGATTGGCGGCGATG
-	1 1	R: CCACAGCGGCTTTAACCAG
G200 RS0114400	Conjugal transfer protein TraF	F: GGCTACACCGATACTTACCAGA
_		R: CACGATAACCACCACGCAA
G200_RS0103275	HlyD family secretion protein	F: AAACCCGCATCAACCCAC
		R: ATCACGCTTCACCTCATCCT
G200_RS0103290	Hemagglutinin	F: CCTGTTGCTGGGTTCATTGTT
		R: GTGGTGGTAGCCGAGGTTT
G200_RS0123635	Transcriptional regulator, TetR family	F: GCAGTCACAGGATGCGATTC
		R: TGAGCCATACACCAGCGATAG
G200_RS0123645	TIM-barrel signal transduction protein	F: CGCTGAAACCGCACTGAAA
		R: GCCGTAGAAACCATCGCAAA
G200_RS0118785	tolI	F: TGGAGAAGGCTGGTCTATTC
		R: GCATTAAAGGGCACAGTGAT
G200_RS0118780	tolR	F: TAATGCGTCTGAAACTGGTC
		R: CGACATATTTCTTCTGCCGA
P. savastanoi pv. sav		
PSA3335_1622	Pyruvate dehydrogenase E1	F: TCAAGGAGCACTGGAATGTCG
	component, beta subunit	R: TCTTCAAGGGATGGAAACGATT
PSA3335_1624	Pyruvate dehydrogenase E1 component	F: CGATACCGTGCTGTGTGTCT
		R: GATCAGGGTGCGGGTAGTTC
PSA3335_1621	LuxR transcriptional regulator	F: ACTGCCCACCGTTGAAGATAA
		R: CATAAGATTTCAGCCAGGAGTCG
PSA3335_2315	Putative hydrocarbon oxygenase	F: TGCCGTTCTTCCTGGCTTA
		R: ACCCGTCATTCATCCACCG
PSA3335_4742	Urocanate hydratase	F: AGCGGGCATTCCTACCTTC
		R: AGAACAACGGGCGGATGTA
PSA3335_1620	Homoserine lactone synthase	F: CACTGACCGAAATGCTGCTGT
		R: TTGCTGACCACCGTGATGAT
PSA3335_4623	Copper chaperone	F: GACTCAAGCGATCAAGAACGATG
		R: CTGCTCGGGTGACAGACTG
PSA3335_2048	Hypothetical protein	F: AATACCACCGCATCGACGAA
		R: TCACGCCGTTGACCAGAAA
PSA3335_0454	Malonate decarboxylase delta subunit	F: TTCGCCAGGCAAGCTATCAA
		R: TCCTCGAAGCCCTGATCCA
PSA3335_2054	Hypothetical protein	F: TGAGCATCTACAGGCTTCGGA
		R:
		CATGTTGATAAGGAATGAGGTTCG
PSA3335_4121	Pectin lyase precursor	F: CCAAGGTGCAGGACTGTTCA
		R: GATACGGGCGAAGGTGTTGT

562 563

30

nline
Ō
Posted
lanuscript
2
Accepted

AEM

564
565

566

	C6-AHL	C8-AHL	3-oxo-C6- AHL	3-oxo-C8- AHL	3-oxo-C10- AHL	3-OH-C6- AHL
PSV	+	-	-	-	-	-
$\Delta pssI$	-	-	-	-	-	-
Δ <i>pssI</i> - pBBR: <i>pssI</i>	+++	+	+++	++	-	-
ET	+++	+	+++	+++	+	++
ETETOI	-	-	-	-	-	-
ETETOI - pBBR: <i>etoI</i>	+++	+++	+++	+++	+++	+++
ETTOLI	+++	+	+++	+++	-	++
ETTOLI- pBBR:tolI	+++	+	+++	+++	-	++

Table 4. Quantification of AHLs produced by PSV NCPPB 3335 and ET DAPP-PG 735<sup>a</sup>

567 568 569

<sup>68</sup> <sup>a</sup>-, no production; +, relative peak area <100,000; ++, relative peak area between 100,000 and 1,000,000;

569 +++, relative peak area >1,000,000

#### 571 Table 5. Genes regulated by pssI in PSV NCPPB 3335

# 572

Locus tag <sup>a</sup>	Gene <sup>b</sup>	Gene product	RNAseq <sup>c</sup>	RT-qPCR <sup>c</sup>
Upregulated				
PSA3335_1622	pdhT	Pyruvate dehydrogenase E1 component, beta subunit	3.27	3.6
PSA3335_1624	pdhQ	Pyruvate dehydrogenase E1 component	2.97	2.32
PSA3335_1621	pssR	LuxR transcriptional regulator	1.44	3.95
Downregulated			•	•
PSA3335_4623	UN	Copper chaperone	-1.07	-0.82
PSA3335_4121	UN	Pectin lyase precursor	-0.92	0.52

<sup>a</sup>Upregulated or downregulated genes in the  $\Delta pssI$  mutant according to RNAseq data.

<sup>b</sup>UN, unnamed

°The log<sub>2</sub> (fold change) obtained in the RNAseq and RT-qPCR experiments are represented. The fold

change refers to the ratio of the average expression obtained in the  $\Delta pssI$  mutant versus the wild type strain

578 in three biological replicates. Genes which QS-dependent expression was corroborated by RT-qPCR are

579 underlined

#### Table 6. Genes regulated by etoI in ET DAPP-PG 735 classified as carbohydrates 580

581 582 metabolism

Gene ID	log <sub>2</sub> (ETEOI/ET)	FDR	Gene product
Inositol catabolism			1
G200_RS0101695	2.56366058	1.13E-09	Major myo-inositol transporter IolT
G200_RS0103410	2.81622077	3.38E-45	Inosose dehydratase IolE
G200_RS0103415	3.051765216	2.74E-47	Glyceraldehyde-3-phosphate ketol-isomerase IolH
G200_RS0103420	3.612129551	3.41E-57	Myo-inositol 2-dehydrogenase 1 IolG
G200_RS0103425	3.034782963	1.24E-11	Epi-inositol hydrolase IolD
G200_RS0103430	2.455264684	4.22E-08	5-keto-2-deoxygluconokinase IolC
G200_RS0103435	1.82595615	7.10E-18	Transcriptional regulator of the myo-inositol catabolic operon IolR
G200_RS0103440	2.322930823	6.16E-29	5-deoxy-glucuronate isomerase IolB
G200_RS0103445	2.343048715	1.92E-08	Methylmalonate-semialdehyde dehydrogenase IolA
G200_RS0103450	2.393433177	3.58E-08	Inosose isomerase IolI
G200_RS0103485	2.265947451	7.57E-22	Inosose dehydratase
G200_RS0103490	1.606575527	5.42E-13	Myo-inositol 2-dehydrogenase
G200_RS0109945 2.054104613		1.56E-06	Myo-inositol 2-dehydrogenase
G200_RS0111735	2.826752946	1.30E-21	Major myo-inositol transporter IolT
G200_RS0119935	2.36064358	6.17E-31	Inositol transport system permease protein
G200_RS0119940	2.922693363	5.94E-43	Inositol transport system ATP-binding protein
G200_RS0119945	2.723773939	6.09E-34	Inositol transport system sugar-binding protein
G200_RS0120045	2.507147476	1.44E-09	Myo-inositol 2-dehydrogenase 2
D-galactarate, D-gluc	arate and D-glycerate	catabolism	1
G200_RS0114355	-1.471923639	1.25E-06	MFS transporter
G200_RS0124280	-2.146858379	7.57E-39	D-galactarate dehydratase GarD
G200_RS0124290	-2.155286292	3.22E-65	D-glucarate permease
G200_RS0124295	-1.762097381	2.90E-22	Glucarate dehydratase GudD
G200_RS0124300	-1.801096855	3.95E-16	Glucarate dehydratase GudD
G200_RS0124305	-1.841655614	7.57E-39	2-dehydro-3-deoxyglucarate aldolase GarL
G200_RS0124320	-1.921850417	2.06E-49	Glycerate kinase
G200_RS25820	-2.073060541	9.97E-53	3-hydroxyisobutyrate dehydrogenase GarR
Maltose and Maltode	xtrin catabolism	- 1	1
G200_RS0105520	-1.474187006	1.51E-22	PTS system, maltose and glucose-specific IIABC component
G200_RS0114455	-2.146215061	6.10E-08	Maltose/maltodextrin high-affinity receptor LamB
G200_RS0114460	-3.460976388	1.17E-46	Maltose/maltodextrin transport ATP-binding protei MalK

G200_RS0114465	-3.432632153		3.66E-	74	Maltose/maltodextrin ABC transporter, substrate binding periplasmic protein MalE	
G200_RS0114470	-1.356395147		1.92E-	06	Maltose ABC transporter permease MalF	
Other carbohydrates	s metabolism				1	
G200_RS0102345	-1.326068817		1.39E-19		6-phospho-beta-glucosidase	
G200_RS0120860	-1.385897754		2.78E-	07	PTS beta-glucoside transporter subunit EIIBCA	
G200_RS0109880	1.195365256		3.02E-	14	Beta-glucuronidase	
G200_RS0108005	1.553737025		2.47E-	29	Alcohol dehydrogenase	
G200_RS0118365	1.430810069		6.79E-	14	Pyruvate formate-lyase	
G200_RS0108900	1.148093171		1.24E-	10	Deoxyribose-phosphate aldolase	
G200_RS0116155	1.055489576		4.73E-	12	Ribokinase	
G200_RS0109855	1.1278524		1.96E-	13	Mannonate dehydratase	
G200_RS0102390	2.327906926		3.00E-	11	Gluconate 2-dehydrogenase, membrane-bound	
G200_RS0102395	2.004607764		1.22E-	17	flavoprotein Gluconate 2-dehydrogenase, membrane-bound, gamma subunit	
G200_RS0119505	1.507781586		2.74E-	15	Ribose ABC transport system, periplasmic ribose-binding protein RbsB	
G200_RS0118360	1.344548034		3.43E-	28	Pyruvate formate lyase 1-activating protein PfIA	
G200_RS0121040	1.68097694		2.43E-	04	Aerobic glycerol-3-phosphate dehydrogenase GlpD	
G200_RS0121025	-1.369452767		7.02E-22		Glucose-1-phosphate adenylyltransferase GlgC	
G200_RS0121030	-1.413808857		4.42E-	26	Glycogen synthase GlgA	
G200_RS0108965	1.651181716		2.59E-	16	6-phosphofructokinase	
G200_RS0105430	-1.010271981		3.98E-	16	Aconitate hydratase AcnA	
G200_RS0114595	-1.302381077		1.85E-	17	Malate synthase	
G200_RS0101545	-2.502124169		2.13E-	42	L-lactate dehydrogenase	
G200_RS0109845	1.012221802		6.78E-	09	MFS transporter LacY	
G200_RS0118000	1.499549769		9.33E-05		6-phosphogluconolactonase	
G200_RS0100900	-1.050323621		2.49E-	14	DUF485 domain-containing protein	
G200_RS0100905	-1.143638292		2.68E-11		Cation/acetate symporter ActP	
G200_RS0121020	-1.529478972		2.20E-39		Glycogen debranching enzyme	
G200_RS0113990	1.292475653		5.30E-11		PTS sugar transporter subunit IIB	
G200_RS0113995	1.209666009		1.43E-15		Putative carbohydrate PTS system, IIA component	
G200_RS0114000	1.458640254		1.69E-13		Putative transcriptional regulator of unknown carbohydrate utilization cluster, GntR family	
G200_RS0104280	-1.044495518		3.39E-	06	Alpha/beta hydrolase	
Gene ID	log <sub>2</sub> (ETEOI/ET	FDR	ł	Ger	e product	
Inositol catabolism	)	1				
G200_RS010169 5	2.56366058	1.13	E-09	Maj	or myo-inositol transporter IolT	
G200_RS010341	2.81622077	3.38	E-45	Inos	sose dehydratase IolE	

G200_RS010341 5	3.051765216	2.74E-47	Glyceraldehyde-3-phosphate ketol-isomerase IolH
G200_RS010342	3.612129551	3.41E-57	Myo-inositol 2-dehydrogenase 1 IolG
G200_RS010342 5	3.034782963	1.24E-11	Epi-inositol hydrolase IolD
G200_RS010343	2.455264684	4.22E-08	5-keto-2-deoxygluconokinase IolC
G200_RS010343	1.82595615	7.10E-18	Transcriptional regulator of the myo-inositol catabolic operon IolR
G200_RS010344	2.322930823	6.16E-29	5-deoxy-glucuronate isomerase IolB
G200_RS010344	2.343048715	1.92E-08	Methylmalonate-semialdehyde dehydrogenase IolA
G200_RS010345	2.393433177	3.58E-08	Inosose isomerase IoII
G200_RS010348	2.265947451	7.57E-22	Inosose dehydratase
G200_RS010349	1.606575527	5.42E-13	Myo-inositol 2-dehydrogenase
G200_RS010994	2.054104613	1.56E-06	Myo-inositol 2-dehydrogenase
G200_RS011173	2.826752946	1.30E-21	Major myo-inositol transporter IolT
G200_RS011993	2.36064358	6.17E-31	Inositol transport system permease protein
G200_RS011994	2.922693363	5.94E-43	Inositol transport system ATP-binding protein
G200_RS011994	2.723773939	6.09E-34	Inositol transport system sugar-binding protein
G200_RS012004	2.507147476	1.44E-09	Myo-inositol 2-dehydrogenase 2
D-galactarate, D-gl	ucarate and D-glyce	rate catabolisr	n
G200_RS011435 5	-1.471923639	1.25E-06	MFS transporter
G200_RS012428	-2.146858379	7.57E-39	D-galactarate dehydratase GarD
G200_RS012429 0	-2.155286292	3.22E-65	D-glucarate permease
G200_RS012429	-1.762097381	2.90E-22	Glucarate dehydratase GudD
G200_RS012430	-1.801096855	3.95E-16	Glucarate dehydratase GudD
G200_RS012430 5	-1.841655614	7.57E-39	2-dehydro-3-deoxyglucarate aldolase GarL
G200_RS012432	-1.921850417	2.06E-49	Glycerate kinase
G200_RS25820	-2.073060541	9.97E-53	3-hydroxyisobutyrate dehydrogenase GarR
Maltose and Maltoo	lextrin catabolism		
G200_RS010552 0	-1.474187006	1.51E-22	PTS system, maltose and glucose-specific IIABC component
G200_RS011445 5	-2.146215061	6.10E-08	Maltose/maltodextrin high-affinity receptor LamB
G200_RS011446 0	-3.460976388	1.17E-46	Maltose/maltodextrin transport ATP-binding protein MalK
G200_RS011446 5	-3.432632153	3.66E-74	Maltose/maltodextrin ABC transporter, substrate binding periplasmic protein MalE
G200_RS011447 0	-1.356395147	1.92E-06	Maltose ABC transporter permease MalF

Other carbohydrate	s metabolism				
G200_RS010234 5	-1.326068817 1.39E-19		6-phospho-beta-glucosidase		
G200_RS012086 0	6 -1.385897754 2.75		PTS beta-glucoside transporter subunit EIIBCA		
G200_RS010988 0	1.195365256	3.02E-14	Beta-glucuronidase		
G200_RS010800 5	1.553737025	2.47E-29	Alcohol dehydrogenase		
G200_RS011836 5	1.430810069	6.79E-14	Pyruvate formate-lyase		
G200_RS010890 0	1.148093171	1.24E-10	Deoxyribose-phosphate aldolase		
G200_RS011615 5	1.055489576	4.73E-12	Ribokinase		
G200_RS010985 5	1.1278524	1.96E-13	Mannonate dehydratase		
G200_RS010239 0	2.327906926	3.00E-11	Gluconate 2-dehydrogenase, membrane-bound, flavoprotein		
G200_RS010239 5	2.004607764	1.22E-17	Gluconate 2-dehydrogenase, membrane-bound, gamma subunit		
G200_RS011950 5	1.507781586	2.74E-15	Ribose ABC transport system, periplasmic ribose-binding protein RbsB		
G200_RS011836 0	1.344548034	3.43E-28	Pyruvate formate lyase 1-activating protein PfIA		
G200_RS012104 0	1.68097694	2.43E-04	Aerobic glycerol-3-phosphate dehydrogenase GlpD		
G200_RS012102 5	-1.369452767	7.02E-22	Glucose-1-phosphate adenylyltransferase GlgC		
G200_RS012103 0	-1.413808857	4.42E-26	Glycogen synthase GlgA		
G200_RS010896 5	1.651181716	2.59E-16	6-phosphofructokinase		
G200_RS010543 0	-1.010271981	3.98E-16	Aconitate hydratase AcnA		
G200_RS011459 5	-1.302381077	1.85E-17	Malate synthase		
G200_RS010154 5	-2.502124169	2.13E-42	L-lactate dehydrogenase		
G200_RS010984 5	1.012221802	6.78E-09	MFS transporter LacY		
G200_RS011800 0	1.499549769	9.33E-05	6-phosphogluconolactonase		
G200_RS010090 0	-1.050323621	2.49E-14	DUF485 domain-containing protein		
G200_RS010090 5	-1.143638292	2.68E-11	Cation/acetate symporter ActP		
G200_RS012102 0	-1.529478972	2.20E-39	Glycogen debranching enzyme		
G200_RS011399 0	1.292475653	5.30E-11	PTS sugar transporter subunit IIB		
G200_RS011399 5	1.209666009	1.43E-15	Putative carbohydrate PTS system, IIA component		
G200_RS011400 0	1.458640254	1.69E-13	Putative transcriptional regulator of unknown carbohydrate utilization cluster, GntR family		
G200_RS010428 0	-1.044495518	3.39E-06	Alpha/beta hydrolase		
Gene ID	log <sub>2</sub> (ETEOI/ET	FDR	Gene product		

Inositol catabolism			
G200_RS010169	2.56366058	1.13E-09	Major myo-inositol transporter IolT
G200_RS010341	2.81622077	3.38E-45	Inosose dehydratase IolE
G200_RS010341	3.051765216	2.74E-47	Glyceraldehyde-3-phosphate ketol-isomerase IolH
G200_RS010342	3.612129551	3.41E-57	Myo-inositol 2-dehydrogenase 1 IolG
G200_RS010342 5	3.034782963	1.24E-11	Epi-inositol hydrolase IolD
G200_RS010343	2.455264684	4.22E-08	5-keto-2-deoxygluconokinase IolC
G200_RS010343 5	1.82595615	7.10E-18	Transcriptional regulator of the myo-inositol catabolic operon IolR
G200_RS010344	2.322930823	6.16E-29	5-deoxy-glucuronate isomerase IolB
G200_RS010344	2.343048715	1.92E-08	Methylmalonate-semialdehyde dehydrogenase IolA
G200_RS010345	2.393433177	3.58E-08	Inosose isomerase IoII
G200_RS010348	2.265947451	7.57E-22	Inosose dehydratase
G200_RS010349	1.606575527	5.42E-13	Myo-inositol 2-dehydrogenase
G200_RS010994	2.054104613	1.56E-06	Myo-inositol 2-dehydrogenase
G200_RS011173	2.826752946	1.30E-21	Major myo-inositol transporter IolT
G200_RS011993	2.36064358	6.17E-31	Inositol transport system permease protein
G200_RS011994	2.922693363	5.94E-43	Inositol transport system ATP-binding protein
G200_RS011994	2.723773939	6.09E-34	Inositol transport system sugar-binding protein
G200_RS012004	2.507147476	1.44E-09	Myo-inositol 2-dehydrogenase 2
D-galactarate, D-gl	ucarate and D-glyce	rate catabolisr	n
G200_RS011435	-1.471923639	1.25E-06	MFS transporter
G200_RS012428	-2.146858379	7.57E-39	D-galactarate dehydratase GarD
G200_RS012429	-2.155286292	3.22E-65	D-glucarate permease
G200_RS012429	-1.762097381	2.90E-22	Glucarate dehydratase GudD
G200_RS012430	-1.801096855	3.95E-16	Glucarate dehydratase GudD
G200_RS012430 5	-1.841655614	7.57E-39	2-dehydro-3-deoxyglucarate aldolase GarL
G200_RS012432	-1.921850417	2.06E-49	Glycerate kinase
G200_RS25820	-2.073060541	9.97E-53	3-hydroxyisobutyrate dehydrogenase GarR
Maltose and Maltoo	dextrin catabolism		
G200_RS010552 0	-1.474187006	1.51E-22	PTS system, maltose and glucose-specific IIABC component
G200_RS011445 5	-2.146215061	6.10E-08	Maltose/maltodextrin high-affinity receptor LamB

37

G200_RS011446	-3.460976388	1.17E-46	Maltose/maltodextrin transport ATP-binding protein MalK
0 G200 RS011446	-3.432632153	3.66E-74	Maltose/maltodextrin ABC transporter, substrate binding
5		3.00E-74	periplasmic protein MalE
G200_RS011447	-1.356395147	1.92E-06	Maltose ABC transporter permease MalF
Other carbohydrates	s metabolism		
G200_RS010234 5	-1.326068817	1.39E-19	6-phospho-beta-glucosidase
G200_RS012086 0	-1.385897754	2.78E-07	PTS beta-glucoside transporter subunit EIIBCA
G200_RS010988	1.195365256	3.02E-14	Beta-glucuronidase
G200_RS010800 5	1.553737025	2.47E-29	Alcohol dehydrogenase
G200_RS011836 5	1.430810069	6.79E-14	Pyruvate formate-lyase
G200_RS010890 0	1.148093171	1.24E-10	Deoxyribose-phosphate aldolase
G200_RS011615 5	1.055489576	4.73E-12	Ribokinase
G200_RS010985 5	1.1278524	1.96E-13	Mannonate dehydratase
G200_RS010239	2.327906926	3.00E-11	Gluconate 2-dehydrogenase, membrane-bound, flavoprotein
G200_RS010239 5	2.004607764	1.22E-17	Gluconate 2-dehydrogenase, membrane-bound, gamma subunit
G200_RS011950	1.507781586	2.74E-15	Ribose ABC transport system, periplasmic ribose-binding protein RbsB
G200_RS011836 0	1.344548034	3.43E-28	Pyruvate formate lyase 1-activating protein PfIA
G200_RS012104	1.68097694	2.43E-04	Aerobic glycerol-3-phosphate dehydrogenase GlpD
G200_RS012102 5	-1.369452767	7.02E-22	Glucose-1-phosphate adenylyltransferase GlgC
G200_RS012103	-1.413808857	4.42E-26	Glycogen synthase GlgA
G200_RS010896 5	1.651181716	2.59E-16	6-phosphofructokinase
G200_RS010543	-1.010271981	3.98E-16	Aconitate hydratase AcnA
G200_RS011459	-1.302381077	1.85E-17	Malate synthase
G200_RS010154	-2.502124169	2.13E-42	L-lactate dehydrogenase
G200_RS010984	1.012221802	6.78E-09	MFS transporter LacY
G200_RS011800 0	1.499549769	9.33E-05	6-phosphogluconolactonase
G200_RS010090	-1.050323621	2.49E-14	DUF485 domain-containing protein
G200_RS010090	-1.143638292	2.68E-11	Cation/acetate symporter ActP
G200_RS012102	-1.529478972	2.20E-39	Glycogen debranching enzyme
G200_RS011399	1.292475653	5.30E-11	PTS sugar transporter subunit IIB
G200_RS011399	1.209666009	1.43E-15	Putative carbohydrate PTS system, IIA component

G200_RS011400 0	1.458640254	1.69E-13	Putative transcriptional regulator of unknown carbohydrate utilization cluster, GntR family
G200_RS010428 0	-1.044495518	3.39E-06	Alpha/beta hydrolase

584

## 585 References586

586		
587	1.	Bulgarelli D, Schlaeppi K, Spaepen S, Ver Loren van Themaat E, Schulze-Lefert
588		P. 2013. Structure and functions of the bacterial microbiota of plants. Annu Rev
589		Plant Biol 64:807-38.
590	2.	Schlaeppi K, Bulgarelli D. 2015. The plant microbiome at work. Mol Plant
591		Microbe Interact 28:212-7.
592	3.	Fuqua WC, Winans SC, Greenberg EP. 1994. Quorum sensing in bacteria: the
593		LuxR-LuxI family of cell density-responsive transcriptional regulators. J
594		Bacteriol 176:269-75.
595	4.	Miller MB, Bassler BL. 2001. Quorum sensing in bacteria. Annu Rev Microbiol
596		55:165-99.
597	5.	Cha C, Gao P, Chen YC, Shaw PD, Farrand SK. 1998. Production of acyl-
598		homoserine lactone quorum-sensing signals by gram-negative plant-associated
599		bacteria. Mol Plant Microbe Interact 11:1119-29.
600	6.	Danhorn T, Fuqua C. 2007. Biofilm formation by plant-associated bacteria. Annu
601		Rev Microbiol 61:401-22.
602	7.	Gonzalez JE, Marketon MM. 2003. Quorum sensing in nitrogen-fixing rhizobia.
603		Microbiol Mol Biol Rev 67:574-92.
604	8.	Newton JA, Fray RG. 2004. Integration of environmental and host-derived signals
605		with quorum sensing during plant-microbe interactions. Cell Microbiol 6:213-24.
606	9.	Von Bodman SB, Bauer WD, Coplin DL. 2003. Quorum sensing in plant-
607		pathogenic bacteria. Annu Rev Phytopathol 41:455-82.
608	10.	Fuqua C, Parsek MR, Greenberg EP. 2001. Regulation of gene expression by cell-
609		to-cell communication: acyl-homoserine lactone quorum sensing. Annu Rev
610		Genet 35:439-68.
611	11.	Lamichhane JR, Venturi V. 2015. Synergisms between microbial pathogens in
612		plant disease complexes: a growing trend. Front Plant Sci 6:385.
613	12.	Vayssier-Taussat M, Albina E, Citti C, Cosson JF, Jacques MA, Lebrun MH, Le
614		Loir Y, Ogliastro M, Petit MA, Roumagnac P, Candresse T. 2014. Shifting the
615		paradigm from pathogens to pathobiome: new concepts in the light of meta-omics.
616		Front Cell Infect Microbiol 4:29.
617	13.	Venturi V, da Silva DP. 2012. Incoming pathogens team up with harmless
618		'resident' bacteria. Trends Microbiol 20:160-4.
619	14.	Buonaurio R, Moretti C, da Silva DP, Cortese C, Ramos C, Venturi V. 2015. The
620		olive knot disease as a model to study the role of interspecies bacterial
621		communities in plant disease. Front Plant Sci 6:434.
622	15.	Hosni T, Moretti C, Devescovi G, Suarez-Moreno ZR, Fatmi MB, Guarnaccia C,
623		Pongor S, Onofri A, Buonaurio R, Venturi V. 2011. Sharing of quorum-sensing
624		signals and role of interspecies communities in a bacterial plant disease. ISME J
625		5:1857-70.
626	16.	Passos da Silva D, Castaneda-Ojeda MP, Moretti C, Buonaurio R, Ramos C,
627		Venturi V. 2014. Bacterial multispecies studies and microbiome analysis of a
628		plant disease. Microbiology 160:556-66.

629	17.	Perez-Martinez I, Rodriguez-Moreno L, Matas IM, Ramos C. 2007. Strain
630		selection and improvement of gene transfer for genetic manipulation of
631		Pseudomonas savastanoi isolated from olive knots. Res Microbiol 158:60-9.
632	18.	Perez-Martinez I, Rodriguez-Moreno L, Lambertsen L, Matas IM, Murillo J,
633		Tegli S, Jimenez AJ, Ramos C. 2010. Fate of a Pseudomonas savastanoi pv.
634		savastanoi type III secretion system mutant in olive plants (Olea europaea L.).
635		Appl Environ Microbiol.
636	19.	Rodriguez-Palenzuela P, Matas IM, Murillo J, Lopez-Solanilla E, Bardaji L,
637		Perez-Martinez I, Rodriguez-Moskera ME, Penyalver R, Lopez MM, Quesada JM,
638		Biehl BS, Perna NT, Glasner JD, Cabot EL, Neeno-Eckwall E, Ramos C. 2010.
639		Annotation and overview of the Pseudomonas savastanoi pv. savastanoi NCPPB
640		3335 draft genome reveals the virulence gene complement of a tumour-inducing
641		pathogen of woody hosts. Environ Microbiol 12:1604-1620.
642	20.	Subramoni S, Florez Salcedo DV, Suarez-Moreno ZR. 2015. A bioinformatic
643		survey of distribution, conservation, and probable functions of LuxR solo
644		regulators in bacteria. Front Cell Infect Microbiol 5:16.
645	21.	Subramoni S, Venturi V. 2009. LuxR-family 'solos': bachelor sensors/regulators
646		of signalling molecules. Microbiology 155:1377-85.
647	22.	Moretti C, Cortese C, Passos da Silva D, Venturi V, Ramos C, Firrao G,
648		Buonaurio R. 2014. Draft Genome Sequence of Pseudomonas savastanoi pv.
649		savastanoi Strain DAPP-PG 722, Isolated in Italy from an Olive Plant Affected by
650		Knot Disease. Genome Announc 2.
651	23.	Moretti C, Cortese C, Passos da Silva D, Venturi V, Torelli E, Firrao G,
652		Buonaurio R. 2014. Draft Genome Sequence of a Hypersensitive Reaction-
653		Inducing Pantoea agglomerans Strain Isolated from Olive Knots Caused by
654		Pseudomonas savastanoi pv. savastanoi. Genome Announc 2.
655	24.	Bartoli C, Carrere S, Lamichhane JR, Varvaro L, Morris CE. 2015. Whole-
656		Genome Sequencing of 10 Pseudomonas syringae Strains Representing Different
657		Host Range Spectra. Genome Announc 3.
658	25.	Thakur S, Weir BS, Guttman DS. 2016. Phytopathogen Genome Announcement:
659		Draft Genome Sequences of 62 Pseudomonas syringae Type and Pathotype
660		Strains. Mol Plant Microbe Interact 29:243-6.
661	26.	Passos da Silva D, Devescovi G, Paszkiewicz K, Moretti C, Buonaurio R,
662		Studholme DJ, Venturi V. 2013. Draft Genome Sequence of Erwinia toletana, a
663		Bacterium Associated with Olive Knots Caused by Pseudomonas savastanoi pv.
664		Savastanoi. Genome Announc 1:e00205-13.
665	27.	Huynh TV, Dahlbeck D, Staskawicz BJ. 1989. Bacterial blight of soybean:
666		regulation of a pathogen gene determining host cultivar specificity. Science
667		245:1374-7.
668	28.	Yu X, Lund SP, Greenwald JW, Records AH, Scott RA, Nettleton D, Lindow SE,
669		Gross DC, Beattie GA. 2014. Transcriptional analysis of the global regulatory
670		networks active in Pseudomonas syringae during leaf colonization. MBio
671		5:e01683-14.
672	29.	Venturi V, Passos da Silva D. 2012. Incoming pathogens team up with harmless
(7)		(m, 1, 1, m, 2, 1, 1, 1, 1, 1, 1, 1, 1, 1, 1, 1, 1, 1,

673 'resident' bacteria. Trends Microbiol 20:160-164.

AEM

Downloaded from http://aem.asm.org/ on August 22, 2018 by guest

674	30.	Deng X, Xiao Y, Lan L, Zhou JM, Tang X. 2009. Pseudomonas syringae pv.
675		phaseolicola mutants compromised for type III secretion system gene induction.
676		Mol Plant Microbe Interact 22:964-76.
677	31.	Quinones B, Pujol CJ, Lindow SE. 2004. Regulation of AHL production and its
678		contribution to epiphytic fitness in Pseudomonas syringae. Mol Plant Microbe
679		Interact 17:521-31.
680	32.	Chalupowicz L, Barash I, Panijel M, Sessa G, Manulis-Sasson S. 2009.
681		Regulatory interactions between quorum-sensing, auxin, cytokinin, and the Hrp
682		regulon in relation to gall formation and epiphytic fitness of <i>Pantoea</i>
683		agglomerans pv. gypsophilae. Mol Plant Microbe Interact 22:849-56.
684	33.	Dulla G, Lindow SE. 2008. Quorum size of <i>Pseudomonas syringae</i> is small and
685		dictated by water availability on the leaf surface. Proc Natl Acad Sci U S A
686		105:3082-7.
687	34.	Whitehead NA, Barnard AM, Slater H, Simpson NJ, Salmond GP. 2001.
688	51.	Quorum-sensing in Gram-negative bacteria. FEMS Microbiol Rev 25:365-404.
689	35.	Cheng F, Ma A, Luo J, Zhuang X, Zhuang G. 2017. N-acylhomoserine lactone-
690	55.	regulation of genes mediating motility and pathogenicity in <i>Pseudomonas</i>
691		syringae pathovar tabaci 11528. Microbiologyopen 6.
692	36.	Scott RA, Lindow SE. 2016. Transcriptional control of quorum sensing and
693	50.	associated metabolic interactions in <i>Pseudomonas syringae</i> strain B728a. Mol
694		Microbiol 99:1080-98.
695	37.	Barnard AM, Salmond GP. 2007. Quorum sensing in <i>Erwinia</i> species. Anal
695 696	57.	Bioanal Chem 387:415-23.
697	38.	Sibanda S, Theron J, Shyntum DY, Moleleki LN, Coutinho TA. 2016.
698	56.	Characterization of two LuxI/R homologs in <i>Pantoea ananatis</i> LMG 2665T. Can
699		J Microbiol 62:893-903.
700	39.	
700	39.	Zheng H, Mao Y, Zhu Q, Ling J, Zhang N, Naseer N, Zhong Z, Zhu J. 2015. The
		quorum sensing regulator CinR hierarchically regulates two other quorum sensing
702		pathways in ligand-dependent and -independent fashions in <i>Rhizobium etli</i> . J
703	40	Bacteriol 197:1573-81.
704	40.	Mattiuzzo M, Bertani I, Ferluga S, Cabrio L, Bigirimana J, Guarnaccia C, Pongor
705		S, Maraite H, Venturi V. 2011. The plant pathogen Pseudomonas fuscovaginae
706		contains two conserved quorum sensing systems involved in virulence and
707		negatively regulated by RsaL and the novel regulator RsaM. Environ Microbiol
708		13:145-62.
709	41.	Liu X, Jia J, Popat R, Ortori CA, Li J, Diggle SP, Gao K, Camara M. 2011.
710		Characterisation of two quorum sensing systems in the endophytic Serratia
711		plymuthica strain G3: differential control of motility and biofilm formation
712		according to life-style. BMC Microbiol 11:26.
713	42.	Venturi V. 2006. Regulation of quorum sensing in Pseudomonas. FEMS
714		Microbiol Rev 30:274-91.
715	43.	Barka EA, Belarbi A, Hachet C, Nowak J, Audran JC. 2000. Enhancement of in
716		vitro growth and resistance to gray mould of Vitis vinifera co-cultured with plant
717		growth-promoting rhizobacteria. FEMS Microbiol Lett 186:91-5.
718	44.	Hubbard BK, Koch M, Palmer DR, Babbitt PC, Gerlt JA. 1998. Evolution of
719		enzymatic activities in the enolase superfamily: characterization of the (D)-

AEM

720		glucarate/galactarate catabolic pathway in Escherichia coli. Biochemistry
721		37:14369-75.
722	45.	Miller JH. 1972. Experiments in molecular genetics, Cold Spring Harbor, N.Y.
723	46.	Hanahan D. 1983. Studies on transformation of <i>Escherichia coli</i> with plasmids. J
724		Mol Biol 166:557-80.
725	47.	Sambrook J, Fritsch EF, Maniatis T. 1989. Molecular cloning: a laboratory
726		manual, 2nd ed., Cold Spring Harbor, N.Y.
727	48.	Matas IM, Castaneda-Ojeda MP, Aragon IM, Antunez-Lamas M, Murillo J,
728		Rodriguez-Palenzuela P, Lopez-Solanilla E, Ramos C. 2014. Translocation and
729		functional analysis of Pseudomonas savastanoi pv. savastanoi NCPPB 3335 type
730		III secretion system effectors reveals two novel effector families of the
731		Pseudomonas syringae complex. Mol Plant Microbe Interact 27:424-36.
732	49.	Aragon IM, Perez-Martinez I, Moreno-Perez A, Cerezo M, Ramos C. 2014. New
733		insights into the role of indole-3-acetic acid in the virulence of Pseudomonas
734		savastanoi pv. savastanoi. FEMS Microbiol Lett 356:184-92.
735	50.	Alexeyev MF. 1999. The pKNOCK series of broad-host-range mobilizable
736		suicide vectors for gene knockout and targeted DNA insertion into the
737		chromosome of gram-negative bacteria. Biotechniques 26:824-6, 828.
738	51.	Coutinho BG, Mitter B, Talbi C, Sessitsch A, Bedmar EJ, Halliday N, James EK,
739		Camara M, Venturi V. 2013. Regulon studies and in planta role of the BraI/R
740		quorum sensing system in the plant beneficial Burkholderia cluster. Appl Environ
741		Microbiol 79:4421-4432.
742	52.	Spaink HP, Okker RJH, Wijffelmann CA, Pees E, Lugtemberg BJJ. 1987.
743		Promoter in the nodulation region of the Rhizobium leguminosarum Sym plasmid
744		pRL1JI. Plant Mol Biol 9:27-39.
745	53.	Uzelac G, Patel HK, Devescovi G, Licastro D, Venturi V. 2017. Quorum sensing
746		and RsaM regulons of the rice pathogen Pseudomonas fuscovaginae.
747		Microbiology in press.
748	54.	Choi SK, Matsuda S, Hoshino T, Peng X, Misawa N. 2006. Characterization of
749		bacterial beta-carotene 3,3'-hydroxylases, CrtZ, and P450 in astaxanthin
750		biosynthetic pathway and adonirubin production by gene combination in
751		Escherichia coli. Appl Microbiol Biotechnol 72:1238-46.
752	55.	Vezzi F, Del Fabbro C, Tomescu AI, Policriti A. 2012. rNA: a fast and accurate
753		short reads numerical aligner. Bioinformatics 28:123-4.
754	56.	Altschul SF, Gish W, Miller W, Myers EW, Lipman DJ. 1990. Basic local
755		alignment search tool. J Mol Biol 215:403-10.
756	57.	Trapnell C, Hendrickson DG, Sauvageau M, Goff L, Rinn JL, Pachter L. 2013.
757		Differential analysis of gene regulation at transcript resolution with RNA-seq. Nat
758		Biotechnol 31:46-53.
759	58.	Trapnell C, Roberts A, Goff L, Pertea G, Kim D, Kelley DR, Pimentel H,
760		Salzberg SL, Rinn JL, Pachter L. 2012. Differential gene and transcript
761		expression analysis of RNA-seq experiments with TopHat and Cufflinks. Nat
762		Protoc 7:562-78.
763	59.	Benjamini Y, Hochberg Y. 1995. Controlling the false discovery rate: a practical
703		belgammin f, however, the method is a Developer for the former of the second se

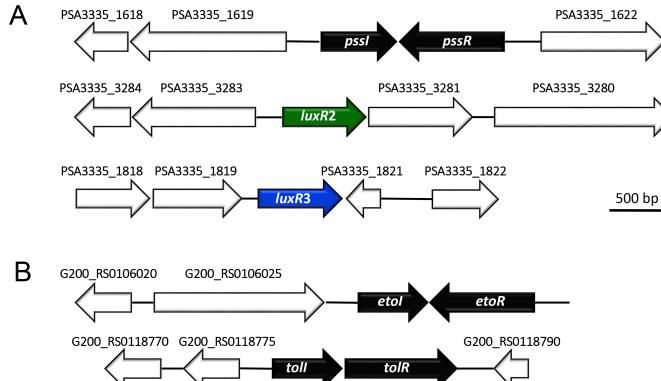
- and powerful approach to multiple testing J Royal Stat Soc 57:289-300.
- 764

AEM

765	60.	Thornton B, Basu C. 2011. Real-time PCR (qPCR) primer design using free
766		online software. Biochem Mol Biol Educ 39:145-54.
767	61.	Livak KJ, Schmittgen TD. 2001. Analysis of relative gene expression data using
768		real-time quantitative PCR and the 2(-Delta Delta C(T)) Method. Methods
769		25:402-8.
770	62.	Rodriguez-Moreno L, Barcelo-Munoz A, Ramos C. 2008. In vitro analysis of the
771		interaction of <i>Pseudomonas savastanoi</i> pvs. savastanoi and nerii with
772		micropropagated olive plants. Phytopathology 98:815-22.
773	63.	Matas IM, Lambertsen L, Rodriguez-Moreno L, Ramos C. 2012. Identification of
774		novel virulence genes and metabolic pathways required for full fitness of
775		Pseudomonas savastanoi pv. savastanoi in olive (Olea europaea) knots. New
776		Phytol 196:1182-96.
777	64.	Penyalver R, Garcia A, Ferrer A, Bertolini E, Quesada JM, Salcedo CI, Piquer J,
778		Perez-Panades J, Carbonell EA, Del Rio C, Caballero JM, Lopez MM. 2006.
779		Factors affecting Pseudomonas savastanoi pv. savastanoi plant Inoculations and
780		their use for evaluation of olive cultivar susceptibility. Phytopathology 96:313-9.
781	65.	Moretti C, Ferrante P, Hosni T, Valentini F, D'Onghia A, Fatmi M, Buonaurio R.
782		2008. Characterization of Pseudomonas savastanoi pv. savastanoi strains
783		collected from olive trees from different countries. In M'Barek Fatmi AC, Nicola
784		Sante Iacobellis, John W. Mansfield, Jesus Murillo, Norman W. Schaad and
785		Matthias Ullrich (ed), Pseudomonas syringae Pathovars and Related Pathogens -
786		Identification, Epidemiology and Genomics. Springer Netherlands.
787	66.	Simon R, Priefer U, Puhler A. 1983. A broad host range mobilization system for
788		in vivo genetic engineering: transposon mutagenesis in Gram negative bacteria.
789		Nat Biotech 1:784-791.
790	67.	Rodriguez-Moreno L, Jimenez AJ, Ramos C. 2009. Endopathogenic lifestyle of
791		Pseudomonas savastanoi pv. savastanoi in olive knots. Microb Biotechnol 2:476-
792		488.
793		

794

Downloaded from http://aem.asm.org/ on August 22, 2018 by guest

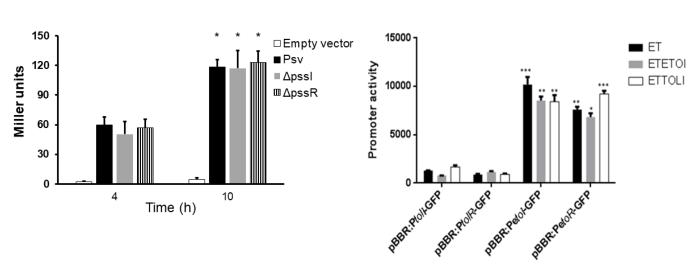


Applied and Environmental Microbiology



A





В

4<sub>7</sub>

2

0

-2

-4

-6

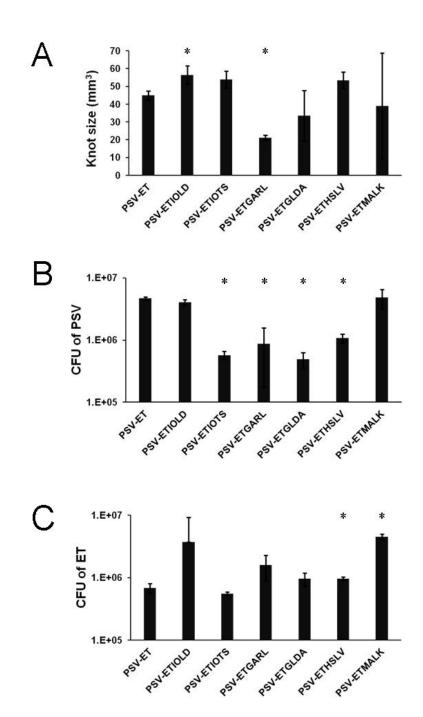
-8

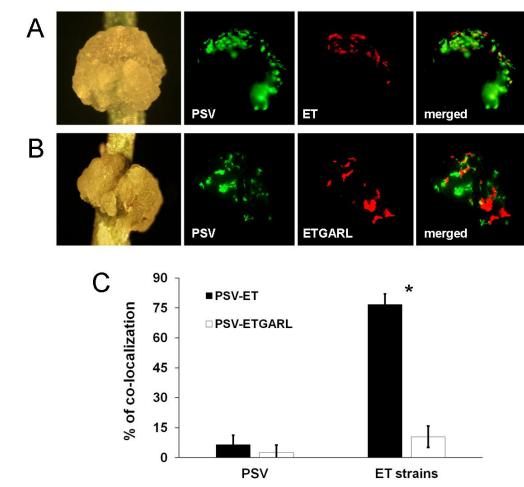
 $\begin{array}{c} -8^{-1} &$ 

log<sub>2</sub>(ETEOI/ET)



ļ





Applied and Environmental Microbiology

Applied and Environmental Microbiology

AEM